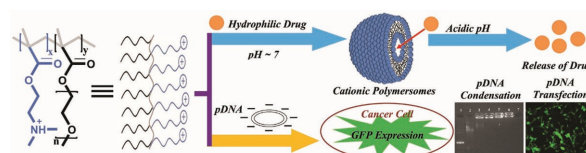


In Vitro Drug and Gene Delivery Using Random Cationic Copolymers Forming Stable and pH-Sensitive Polymersomes

Partha Laskar, Joykrishna Dey,* Payel Banik, Mahitosh Mandal, Sudip Kumar Ghosh

Stimuli-sensitive polymeric vesicles or polymersomes as self-assembled colloidal nanocarriers have received paramount importance for their integral role as delivery system for therapeutics and biotherapeutics. This work describes spontaneous polymersome formation at pH 7, as evidenced by surface tension, steady state fluorescence, dynamic light scattering, and microscopic studies, by three hydrophilic random cationic copolymers synthesized using *N,N*-(dimethylamino)ethyl methacrylate (DMAEM) and methoxy poly(ethylene glycol) monomethacrylate in different mole ratios. The results suggest that methoxy poly(ethylene glycol) chains constitute the bilayer membrane of the polymersomes and DMAEM projects toward water constituting the positively charged surface. The polymersomes have been observed to release their encapsulated guest at acidic pH as a result of transformation into polymeric micelles. All these highly biocompatible cationic polymers show successful gene transfection ability as nonviral vector on human cell line with different potential. Thus these polymers prove their utility as a potential delivery system for hydrophilic model drug as well as genetic material.



1. Introduction

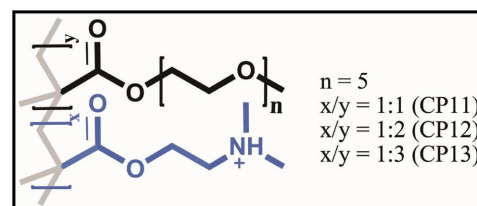
Polymers are one of the utility materials due to their vast applications in material and biological science.

Dr. P. Laskar, Prof. J. Dey
Department of Chemistry
Indian Institute of Technology Kharagpur
Kharagpur 721 302, India
E-mail: joydey@chem.iitkgp.ernet.in
P. Banik, Prof. M. Mandal
School of Medical Science and Technology
Indian Institute of Technology Kharagpur
Kharagpur 721 302, India
Prof. S. K. Ghosh
Department of Biotechnology
Indian Institute of Technology Kharagpur
Kharagpur 721 302, India

Self-assembled polymers are being considered as one of the smartest colloidal materials due to their wide variety of morphologies and potential application in delivery of drugs, pharmaceutical agents, and genetic materials.^[1–6] Additional features like incorporated stimuli-sensitive functionality, high molecular weight, assemblies with large surface area, and long circulatory lifetime have made biocompatible polymers as one of the most attractive drug delivery systems (DDSs).^[7–11] Polymers may self-assemble into various nanostructures in water, such as spherical micelles, cylindrical micelles, lamella, vesicles, etc., depending on its molecular weight, hydrophilic-lipophilic balance, chemical structure, concentration, and external stimuli (ratio of organic solvent/water composition, ionic strength, pH, temperature, etc.).^[2,12–14] Polymersomes (PSs) or polymeric vesicles are an important class of polymeric self-assembly that has a paramount impetus

and play an integral role in the development of DDSs.^[11–18] Vesicles are self-assemblies with an aqueous core separated from the outside aqueous media by a hydrophobic bilayer membrane. Consequently, unlike micelles or nanoparticles, they not only can encapsulate hydrophobic guests in their bilayer membrane, but also can encapsulate hydrophilic cargos within their aqueous core.^[15,18,19] The application of PSs becomes more important when the constituent polymer is tailored with groups sensitive to various stimuli, such as pH, temperature, redox reaction, and ionic strength, because they trigger the release of the encapsulated guest.^[20–23] Among these, the pH-sensitive delivery systems are particularly more demanding for biological applications as large pH variations are observed in different parts of human body, for example, in the inflamed cells, particularly cancerous cells which thrive in acidic environment.^[24] Thus, along with biocompatibility and encapsulation capacity, pH-responsiveness also increases the efficiency of PSs by releasing the guest at the target site, particularly at the cancerous cell having acidic pH. Different types of cationic polymers have also drawn tremendous interest in nonviral gene delivery for their successful condensing and targeting ability for nucleic acid or any other genetic materials.^[25–34] Therefore, stimuli-sensitive polymeric nanostructures having cationic groups are now being used for dual mode or code-livery of gene and drug in nanomedicine so that nucleic acid/protein (encapsulated or complexed) can suppress the gene and the drug (conjugated or encapsulated) can cure the disease.^[35–40]

Usually PS formation is reported for block copolymers having a suitable ratio of hydrophilic and hydrophobic blocks in the polymer chain.^[13,15,18] Recently, there are several reports on PS formation by hydrophilic block copolymers, but in stipulated condition.^[41–43] However, spontaneous PS formation without the use of any external stimulus is more acceptable for the development of DDSs. On the other hand, *N,N*-(dimethylamino)ethyl methacrylate (DMAEM) has been successfully used as a pH- and/or temperature-sensitive amphiphilic block to synthesize a large number of cationic block copolymers for use as drug and/or gene delivery vehicle.^[28,35,44–46] In most cases, however, researchers have reported nanoparticles and micelles formation by block copolymers incorporating DMAEM.^[35,47–49] Though Schubert's group in 2012 have reported vesicular assembly formation by block copolymer consisting of DMAEM and oligoethylene glycol, but the microstructures (multilamellar vesicles at 37 °C and unilamellar vesicles at 50 °C) formed only at elevated temperatures.^[50] At 37 °C, methoxy poly(ethylene glycol) (mPEG) formed bilayers of the multilamellar PSs.^[50] Recently, we have also reported vesicle formation by a novel mPEG based cationic low-molecular-weight surfactant, where mPEG formed the bilayer of the vesicle



Scheme 1. General chemical structure of the cationic polymers CP11, CP12, and CP13.

at room temperature.^[51] This work was extended to synthesize a series of random copolymers containing mPEG and L-cysteine that spontaneously formed zwitterionic PSs in aqueous medium.^[52]

In continuation with our earlier work, here we report for the first time, spontaneous formation of cationic PSs in water (pH 7) at room temperature by a series of the so-called hydrophilic and biocompatible cationic random copolymers, poly[(2-(dimethylamino)ethyl methacrylate)_x-co-(methoxy poly(ethylene glycol) methacrylate)_y], poly[DMAEM_x-co-mPEG_y] (see Scheme 1 for structure). The DMAEM and mPEG ($M_n \approx 300$) monomers were polymerized at 1:1, 1:2, and 1:3 feed ratios by use of random polymerization technique to obtain copolymers CP11, CP12, and CP13, respectively (Scheme S1, Supporting Information). The self-assembly behavior of these cationic polymers was studied by surface tension and steady-state fluorescence technique using different fluorescent probes. The morphology of the aggregates was investigated by use of the dynamic light scattering (DLS), and electron and fluorescence microscopy. All three polymers were found to form PS in water at room temperature. Lower critical solution temperature (LCST) of these cationic polymers at different concentrations and pH was also measured to evaluate solution phase stability of the PSs at elevated temperatures. Drug encapsulation and pH-triggered release studies were performed using calcein as a fluorescent dye. Cell viability and hemolysis assays were performed with the polymers to determine their cellular toxicity and blood compatibility, respectively. The interaction of the polymers with human serum albumin (HSA) was investigated using circular dichroism (CD) spectroscopy. In addition to demonstrate the utility of these PSs as DDS, these cationic polymers were also evaluated as potential nonviral vector for gene transfection by condensing and transfecting plasmid DNA (pDNA) into the cellular compartment.

2. Experimental Section

2.1. Materials

Methoxy poly(ethylene glycol) methacrylate (mPEG, $M_n \approx 300$, where $n = 5$), 2-(dimethylamino)ethyl methacrylate (DMAEM),

chloroform-d, HSA of M_w 66.4 kDa, and 3-(4,5-dimethylthiazol-2-yl)-2,5-diphenyl-tetrazolium bromide (MTT) were purchased from Sigma-Aldrich (Bangalore, India) and were used without further purification. Radical initiator, 2,2'-azobis(isobutyronitrile), was purchased from Sigma-Aldrich (Bangalore, India) and was further recrystallized from acetone before use. Fluorescent probes *N*-phenyl-1-naphthyl amine (NPN), pyrene (Py), 1,6-diphenyl-1,3,5-hexatriene (DPH), rhodamine 6G (R6G), calcein (Cal), and ethidium bromide (EB) were purchased from Sigma-Aldrich (Bangalore, India) and were recrystallized from ethanol (EtOH) before use. Solvents like tetrahydrofuran (THF), methanol (MeOH), and acetone were purchased from Merck (Bangalore, India) and were distilled and purified before use. Milli Q (18.2 M Ω) water was obtained from Millipore water purifier (Elix3, Bangalore, India).

2.2. General Instrumentation

A digital pH meter (pH 5652, EC India Ltd., Kolkata) was used to measure the pH of the various solutions. Turbidity of polymer solutions was measured as percent transmittance (%T) using UV-vis-NIR spectrophotometer (Varian, Model-Cary 5000) associated with an automated temperature controller (Cary temperature controller-UV0904M400). The $^1\text{H-NMR}$ spectra were recorded on a Bruker Avance 400 spectrometer operated at 400 MHz using TMS as internal reference standard.

2.3. Gel Permeation Chromatography

Average molecular weight and corresponding polydispersity index (PDI) of polymers were measured by gel permeation chromatography (GPC, Waters 2414, Refractive Index Detector, Waters 515 HPLC PUMP) using THF (HPLC grade) as an eluent at a flow rate of 1.0 mL min $^{-1}$ at 303 K and the injection volume was 100 μL . The molecular weight of the polymers was obtained from a calibration curve constructed using poly(methyl methacrylate) (PMMA) of known molecular weight as standard.

2.4. Surface Tension Measurement

Surface tension (γ mN m $^{-1}$) of each copolymer solution in aqueous media was measured with a surface tensiometer (Model 3S, GBX, France) at 298 K using Du Nuoy ring detachment method. Before every experiment, the platinum-iridium ring was washed with 50% (v/v) EtOH-HCl solution and was burnt in the oxidizing flame. The surface tension of distilled water and phosphate buffer saline (PBS) buffer (pH 7) were measured every time before the experiment started with polymer solutions. For measurements at different concentrations, an aliquot of the stock polymer solution was added to a known volume of water (or buffer) in a teflon beaker and stirred for 25–30 min for equilibration. Surface tension for each polymer concentration was measured in triplicate and an average surface tension value was taken.

2.5. Steady-State Fluorescence Measurement

Steady-state fluorescence spectra of Py and NPN fluorescent probes were measured with a SPEX Fluorolog-3 spectrophotometer.

Stock solutions ($\approx 1.0 \times 10^{-3}$ M) of NPN and Py were prepared first in MeOH and a required amount of this stock solution was added into 5 mL volumetric flasks. After evaporation of methanol under a stream of N $_2$ gas an aliquot of the polymer stock solution was added to the volumetric flask and diluted to 5 mL. The concentrations of NPN and Py were maintained at around 1.0×10^{-5} and 1.0×10^{-6} M, respectively. The mixtures were shaken vigorously for 30 min at room temperature and were kept in a dark place for 12 h for equilibration. The samples containing Py and NPN were excited at 343 and 340 nm, respectively, and the emission spectra were recorded in the wavelength range 350–600 nm. The excitation and emission slit widths were adjusted at 10 and 2 nm, respectively for the measurements of Py fluorescence, while fluorescence spectra of the solutions containing NPN were recorded using both excitation and emission slit width of 5 nm. A Perkin Elmer LS-55 spectrophotometer equipped with a thermostated, water jacketed and magnetically stirred cell holder, and filter polarizer assembly (L-format configuration) was used to measure steady-state fluorescence anisotropy (r) of DPH at 450 nm. For each polymer concentration, an average value of six measurements was noted. For temperature-dependent fluorescence measurements, a Thermo Neslab RTE-7 circulating water bath was used for temperature control within ± 0.1 $^\circ\text{C}$. The solution was allowed to equilibrate for exactly 10 min at the desired temperature.

2.6. Circular Dichroism Spectra

CD spectra of HSA and its complexes with polymers were recorded under N $_2$ atmosphere with a Jasco J-815 spectrometer in the far-UV region (190–270 nm) using a quartz cell of 1 mm path length. The spectrometer was fitted with an automated N $_2$ supplier and a Peltier type temperature controller. Polymer solutions of different concentrations (0.01%, 0.05%, 0.1%, and 0.2%) were made with a fixed HSA (0.1% or 1 g L $^{-1}$ or 15×10^{-6} M) concentration (by weight) for each polymer. The complexes were incubated for about 14–15 h before measurement. An accumulation of two scans with a scan speed 50 nm min $^{-1}$ was performed and data were collected in the wavelength range from 270 to 190 nm at 298 K. The reference CD spectrum of the corresponding polymer solution was taken before every measurement and each spectrum was blank subtracted.

The α -helix content (%) was calculated from the mean residual ellipticity (MRE) which was calculated from the corresponding θ_{obs} value measured at 208 nm (MRE $_{208}$). The α -helix content (%) was calculated using Equations (1) and (2)^[53–55]

$$\text{MRE} = \frac{\theta_{\text{obs}} M}{nlC} \quad (1)$$

$$\alpha\text{-helix}(\%) = \frac{(-\text{MRE}_{208} - 4000)}{(33000 - 4000)} \quad (2)$$

where θ_{obs} is the CD in millidegrees, M is the molecular weight (66.4 kDa) of the HSA protein in g dmol $^{-1}$, n is the number of the amino acid residues (585 in the case of HSA), and l is the path length (1 mm) of the cuvette, and C is the concentration of the protein in g L $^{-1}$. MRE $_{208}$ is the observed MRE value at 208 nm. The MRE value of the β -sheet and random coil conformations at 208 nm is 4000 and that of a pure α -helix is 33 000.

2.7. Dynamic Light Scattering

The DLS technique was employed to measure mean hydrodynamic diameter (d_H) of polymeric aggregates in aqueous media using Malvern Nano ZS (UK) instrument fitted with a 4 mW He-Ne laser ($\lambda = 632.8$ nm) source. Scattering angle in the instrument was fixed at 173° to collect all the scattering photons. Each polymer solution was filtered through a $0.45 \mu\text{m}$ filter paper (Millipore Millex syringe filter) and incubated at 298 K for at least 6 h before measurement. Each sample was allowed to equilibrate for 2 min in the cell holder at 298 K before data collection started. Data analysis was performed using instrumental software. The d_H value of the aggregates was obtained from Stokes-Einstein equation. The DLS measurement for each concentration was repeated three times and mean value of d_H was noted.

2.8. Electron Microscopy

The transmission electron images of the polymer solutions of different concentrations and pH were measured with a high-resolution transmission electron microscope (HRTEM) (JEOL, JEM 2100, Japan) operating at an accelerating voltage of 200 kV. The images were captured using a Charge Couple Device (CCD) camera (Gatan) and the filament was made of LaB₆. A very minute amount ($\approx 5 \mu\text{L}$) of each polymer solution was dropped on a carbon-coated copper grid (400 mesh size), and excess solution was carefully blotted using a filter paper. The samples were then kept in desiccators overnight for drying at room temperature until before measurement. For each polymer concentration, the measurement was repeated at least twice to check reproducibility and thus to eliminate the possibility of any artefacts.

2.9. Agarose Gel Electrophoresis

Agarose gel electrophoresis retardation assay was performed to assess DNA condensation ability of the cationic polymers prior to transfection. A fixed amount of EGFP vector plasmid was incubated with different amount of cationic polymers (in different weight ratios) for 1 h and then the complex solution was mixed with $4 \mu\text{L}$ $6\times$ loading buffer and requisite amount of glycerol before loading into a 1.0 wt% agarose gel containing 0.5 mg mL^{-1} EB. Polymer free EGFP plasmid DNA was loaded in another lane as control. Electrophoresis was set up in TAE buffer at 90 V. After 45 min, the retardation of DNA by the polymers was analyzed on UV transilluminator (Dolphin-DOC^{Plus}, Wealtec) to locate the presence of DNA.

2.10. Hemolytic Assay

Hemocompatibility tests for all three polymers were performed following a standard protocol reported elsewhere.^[56,57] First, the polymers were dissolved completely in PBS of pH 7.4. $\approx 5 \text{ mL}$ of fresh blood was taken before the experiment and then, red blood cells (RBCs) were procured by centrifugation at 3000 rpm for 10 min at room temperature. The collected RBCs were washed four times with $150 \times 10^{-3} \text{ M}$ NaCl solution to remove the serum completely. The final RBC concentration of around $5 \times 10^8 \text{ RBC mL}^{-1}$ was prepared as suspended solution in PBS.

The final RBC suspension ($200 \mu\text{L}$) was mixed properly with the desired amount of polymer solution and the final volume of the mixture was made up to 1 mL with PBS of pH 7.4. RBC suspension in only PBS and mixed with triton X-100 (1%, w/v) were considered as negative and positive control, respectively. All these prepared RBC solutions containing polymer of varying concentrations as well as the controls in the microcentrifuge tubes were then incubated for 60 min at 310 K in a water bath with an intermittent mixing. All samples were then centrifuged at 12 000 rpm for 5 min and the supernatants were collected to measure their absorbance values at 541 nm in ELISA reader (Biorad, USA) using PBS as the blank. For each polymer concentration, measurements were done in triplicate and the mean value was noted.

2.11. Cytotoxicity Assay

MDA-MB-231 cells were cultured in DMEM (Dulbecco's Modified Eagle's Medium) to assess the cell viability or cytotoxicity using a conventional and standard MTT dye reduction assay.^[56,57] Antibiotics solution containing penicillin ($100 \text{ units mL}^{-1}$), 10% fetal bovine serum, amphotericin B ($0.25 \mu\text{g mL}^{-1}$), and streptomycin (0.1 mg mL^{-1}) were supplemented to the cells and then the cells were incubated with a feeding cycle of 48 h at 310 K in T-25 flasks in a 5% CO₂ humidified chamber. After sufficient level of confluency in cells monolayer, it was trypsinized (0.25% Trypsin + 0.1% EDTA) and was harvested by centrifugation at 1500 rpm.

For cytotoxicity assay, the cell suspensions were further seeded in $200 \mu\text{L}$ of complete DMEM in a 96-well plate at a concentration 2×10^3 cells per well. The cells were allowed to adhere and were grown for nearly 16 h at 310 K in a 5% CO₂ humidified incubator. Polymer stock solutions were prepared in incomplete DMEM medium with a 2 h of incubation and filtered through $0.2 \mu\text{m}$ polycarbonate filter just before addition. The medium from the cultured cells in each well was carefully replaced with a total of $200 \mu\text{L}$ of fresh medium containing polymers with the desired concentrations. After 36 h of incubation with the polymers, the medium was removed and cells were washed thrice properly with sterile PBS. Finally, $100 \mu\text{L}$ of MTT reagent (0.5 g L^{-1} in PBS) and $100 \mu\text{L}$ fresh media were added to each well and incubated for 3 h to reduce the MTT to formazan dye by the enzyme of the live cells in each well. Then MTT was removed and $200 \mu\text{L}$ of DMSO was added into each well to solubilize the formazan dye. The amount of formazan dye produced was measured spectrophotometrically at 540 nm. The experiment was performed in triplicate and an average value was obtained. The cytotoxicity was expressed as percentage of cell viability with respect to the untreated (without any addition of polymer) control cells, using Equation (3)

$$\text{Cell viability (\%)} = \left(\frac{\text{Mean of absorbance value of treated cells}}{\text{Mean of absorbance value of untreated control cells}} \right) \times 100 \quad (3)$$

Cytocompatibility of the polyplexes (polymer complexed with pDNA) at different concentrations of the polymer was carried out on the same cell line after 1 h of complexation in the incomplete media. After 36 h of incubation with the polyplexes, the MTT assay was performed.

2.12. Gene Transfection

For the determination of gene transfection, MDA-MB-231 cells were seeded on cover slips and allowed to 70% confluent on the day of plasmid delivery. The pDNA-polymer complexes were prepared by incubating pDNA containing reporter gene which encode green fluorescence protein (GFP) with each of the polymers for 1 h at two weight ratios (pDNA:polymer, 1:50 and 1:100, respectively). The complete cell-growth medium was replaced with incomplete medium just prior to the addition of the complexes. The complexes were added drop wise to the cells kept in incomplete DMEM and were incubated for 8 h in 310 K humidified chamber containing 5% CO₂. After 8 h, the complex-containing medium was replaced by a complete DMEM medium. The expressed GFP fluorescence within the cells was captured by fluorescence microscope (Zeiss Observer Z1, Germany) after 24 h of incubation.

3. Results and Discussion

3.1. Molecular Characterization

The ¹H-NMR spectra (Figures S1–S3, Supporting Information) not only confirmed the chemical structure of the copolymers, but also the peak integrations at the chemical shift positions of –OCH₃ group ($\approx \delta$ 3.38 ppm) of the mPEG chain and –CH₃ group ($\approx \delta$ 2.3 ppm) and –CH₂ group ($\approx \delta$ 2.6 ppm) of DMAEM gave the exact mole ratio of two monomer units in the polymer chain. The mole ratios of DMAEM and mPEG monomers in the polymer were found to be 1:1, 1:2, 1:3 for **CP11**, **CP12**, and **CP13** polymer, respectively. This means the mPEG content of the polymer chain gradually increases in going from **CP11** to **CP13**. The weight-average molecular weight (\bar{M}_w) and PDI of **CP11** (10 330 Da; 1.6), **CP12** (17 455 Da; 1.83), and **CP13** (11 682 Da; 1.4) polymers were determined by conventional GPC technique (Figure S4, Supporting Information) using PMMA as standard.

The copolymers were obtained as uncharged species. However, as a result of protonation of the –N(CH₃)₂ groups, they become positively charged when dissolved in water (pH 7). Consequently, the aqueous solubility of the copolymers is increased. The high %T (\approx 90%) value (Figure S5, Supporting Information) of the polymer solution (\approx 1.0 mg mL⁻¹) suggests good aqueous solubility of copolymers at room temperature (298 K), which is beneficial for application of these polymers as DDS.

3.2. Surface Activity

In order to examine amphiphilic character of the polymers, we performed surface tension (γ mN m⁻¹) measurements of the polymer solutions (pH 7) at different concentrations at 298 K. The data are presented in Figure 1. With all three copolymers, a gradual reduction of γ value of water with

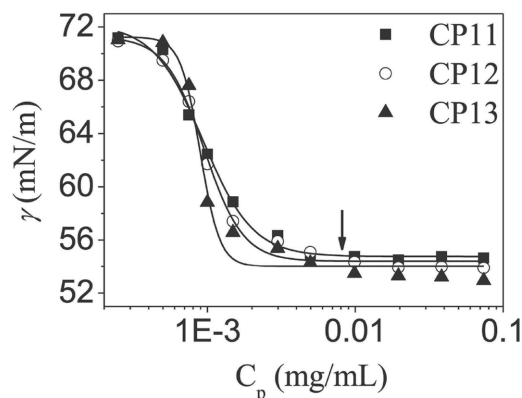


Figure 1. Plots showing variation of surface tension (γ mN m⁻¹) of buffer solution (pH 7) with polymer concentration (C_p) at 298 K.

the increase of polymer concentration (C_p) is evident. The γ value of water reaches a plateau at a concentration of \approx 10 μ g mL⁻¹. The decrease of γ in the presence of polymers is indicative of amphiphilic nature of the copolymers. However, the surface activity of the copolymers is relatively low in comparison to low-molecular-weight monomeric cationic surfactant CTAB and typical hydrophobe-containing copolymers.^[56–58] This means that the copolymers are more polar due to the presence of protonated –N(CH₃)₂ groups and so-called polar mPEG chains. Among these copolymers, **CP13** having maximum mPEG content, shows slightly higher surface activity. However, the feature of the surface tension plots suggests self-association of the polymers in water. Therefore, the C_p value corresponding to the breakpoint in the plot was taken as the critical aggregation concentration (CAC) of the polymer. It is observed that the CAC values (\approx 4 μ g mL⁻¹) of the polymers, within the experimental error limit, are almost equal.

3.3. Self-Association Behavior

In order to study the self-association properties of the amphiphilic copolymers, we employed steady-state fluorescence probe technique and used NPN as a fluorescent probe. Usually NPN is weakly fluorescent in water, but its fluorescence intensity increases along with a blue shift ($\Delta\lambda = \lambda_{\text{water}} - \lambda_{\text{solution}}$) of the emission maxima (λ_{max}) when it is solubilized within nonpolar microenvironment.^[56,57] For all the polymers, a huge blue shift of the λ_{max} value was observed and the shift increased with the increase of C_p following a sigmoid pattern as shown by the fluorescence titration curves (Figure 2a). This indicates incorporation of NPN molecules within the hydrophobic domains formed by the copolymers, which suggests self-aggregation of the copolymers. The concentration independence of $\Delta\lambda$ at low polymer concentrations is indicative of hydrophobic domain formation through inter-chain association. The concentration corresponding to the onset of rise of the

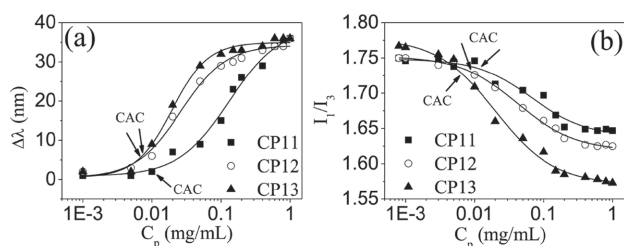


Figure 2. Plots of a) shift ($\Delta\lambda$) fluorescence maximum of NPN and b) I_1/I_3 ratio of Py probe versus polymer concentration (C_p , mg mL^{-1}) at 298 K.

curve (indicated by the downward and upward arrows) can therefore be taken as CAC value. The CAC values thus obtained for **CP11** ($9 \mu\text{g mL}^{-1}$), **CP12** ($7 \mu\text{g mL}^{-1}$), and **CP13** ($7 \mu\text{g mL}^{-1}$) are closely equal and are consistent with the results of surface tension measurements. Despite the absence of typical hydrophobes in their polymeric backbone, all the polymers have relatively lower CAC value. However, it is observed that with the increase of mPEG content (in case of **CP12** and **CP13**) and molecular weight (in case of **CP13**) the CAC value decreases slightly. This is similar to low-molecular-weight surfactants in which the CAC value decreases with the increase of hydrocarbon chain length or hydrophobicity. This means the mPEG chains of the copolymers behave like hydrophobes and form hydrophobic domains.

In support to the results of NPN probe study, we have also carried out fluorescence titration using Py as a probe molecule. Like NPN, Py is also nearly insoluble in water, but gives highly structured fluorescence spectrum. Because of its hydrophobic nature Py gets solubilized within the hydrophobic core of any aggregates as indicated by the change in intensity ratio (I_1/I_3) of the first (I_1) and third (I_3) vibronic peaks of the fluorescence spectrum.^[56,57] Indeed a gradual decrease of the I_1/I_3 ratio with the increase in polymer concentration can be observed (Figure 2b) with all three copolymers. This is consistent with the microdomain formation by the polymer molecules in water. The CAC value was obtained from the concentration corresponding to the onset (indicated by the downward and upward arrows) of fall of I_1/I_3 value in the respective titration curve. The CAC values of **CP11** ($\approx 10 \mu\text{g mL}^{-1}$), **CP12** ($\approx 9 \mu\text{g mL}^{-1}$), **CP13** ($\approx 7 \mu\text{g mL}^{-1}$) thus obtained are similar to the values obtained from fluorescence titrations using NPN probe. However, relatively higher values of I_1/I_3 ratio suggest that the microdomains are slightly polar in

comparison to those of micelles of low-molecular-weight surfactants with hydrocarbon tail. This indicates that the microdomains are constituted by the mPEG chains of the polymer.

In order to determine the fluidity (inverse of viscosity) of the microdomains, we have also employed DPH as a fluorescent probe. DPH is weakly fluorescent in water because of its poor aqueous solubility, but when it is solubilized within hydrophobic microenvironments of micelles or vesicles it shows an enhancement of fluorescence intensity. Further, the steady-state fluorescence anisotropy (r) of DPH in these microenvironments increases due to its restricted rotational motion. Thus r -value of DPH is a measure of the rigidity of microenvironments of aggregates. The r -values of DPH in polymer solutions (1 mg mL^{-1}) were observed to be much higher which increased in the order **CP11** (0.239) < **CP12** (0.276) < **CP13** (0.282), indicating that the microdomains formed by the mPEG chains are very viscous in nature or rigid. The higher rigidity of the bilayer membrane in the case of **CP13** polymer can be attributed to higher mPEG content causing greater entanglement of mPEG chains.

3.4. Morphology of the Aggregates

For drug delivery applications shape or morphology of the self-assembled nanostructures is an important parameter. Therefore, we took HRTEM images of both dilute (Figure 3a) and concentrated (Figure 3b) polymer solutions at room temperature. Figure 3 clearly reveals existence of PSs in aqueous solution of all three copolymers. Indeed PSs of $d_H \approx 50 \text{ nm}$ in both dilute (0.1 mg mL^{-1}) and concentrated (1 mg mL^{-1}) solutions can be seen in the corresponding image. Although the presence of some smaller vesicular

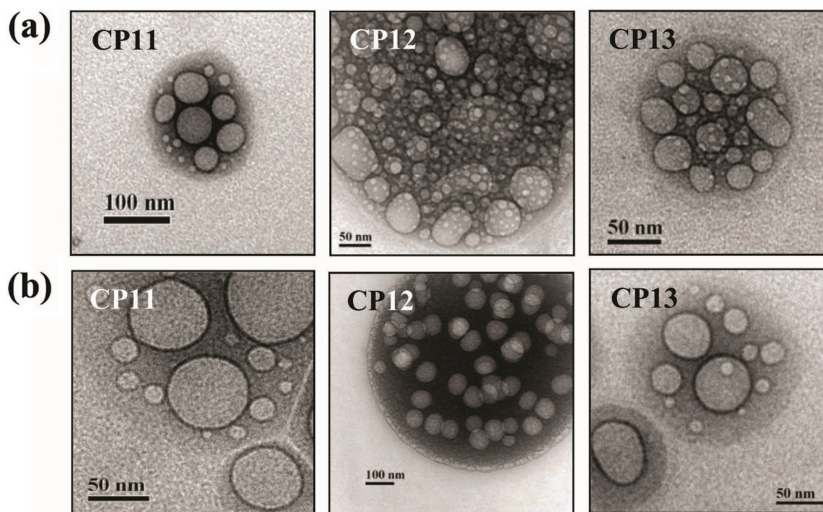


Figure 3. Unstained HRTEM images of **CP11**, **CP12**, and **CP13** copolymers in aqueous media: a) 0.1 mg mL^{-1} and b) 1.0 mg mL^{-1} .

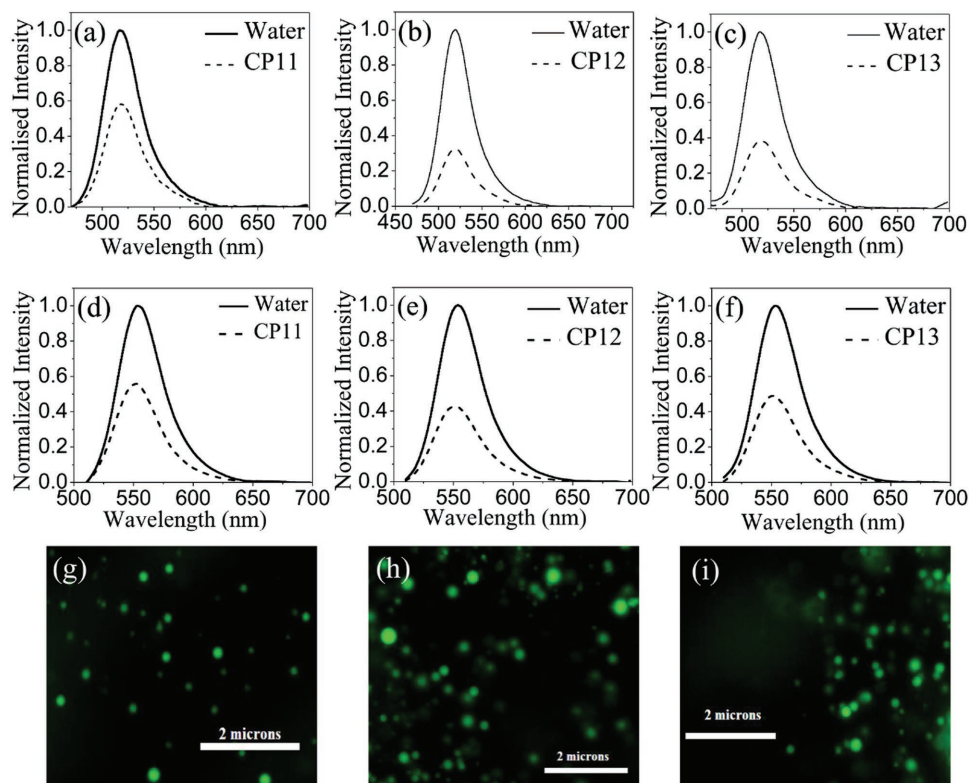


Figure 4. Normalized fluorescence spectra of a–c) Cal and d–f) R6G in pH 7 buffer in the absence (control) and presence of different polymers (0.2 mg mL^{-1}) at 298 K; CFM images of Cal-entrapped PSs: g) CP11, h) CP12, and i) CP13; bar represents $2 \mu\text{m}$.

assemblies ($<50 \text{ nm}$) could be seen, the majority of PSs have mean d_{H} value of $\approx 50 \text{ nm}$. It should be noted that the PS formation occurs spontaneously in aqueous solution of all the polymers.

However, conventional HRTEM images obtained by drying method are often criticized as artefacts. Vesicles can not only encapsulate hydrophobic dye in their bilayer membrane, but can also encapsulate hydrophilic dye in their aqueous core.^[59] Therefore, in order to prove the existence of aqueous core, we have carried out hydrophilic dye entrapment experiment using Cal as a fluorescent dye. The steady-state fluorescence spectra (Figure 4a–c) of encapsulated Cal dye obtained by thorough dialysis of the polymer solutions were measured. It can be observed that the normalized fluorescence emission intensity of Cal-encapsulated PSs is much less in comparison to the fluorescence intensity of the absorbance-matched solution of Cal in water without the polymer (control). The quenching of fluorescence intensity of Cal can be attributed to confinement of the probe molecules into the small volume of the water-filled core of the polymeric vesicles, which increases its effective concentration causing self-quenching of Cal fluorescence.^[59] However, it can be argued that the polymers being positively charged and Cal is a negatively charged dye the observed self-quenching of Cal fluorescence could be due to an additional effect of

increased local concentration due to simple binding of Cal to the surface of PSs. In order to examine this, the same experiment was performed using a cationic hydrophilic dye, R6G which also is known to exhibit self-quenching of fluorescence upon confinement into the vesicle core.^[59] Indeed, the results presented in Figure 4d–f are similar to that of Cal and clearly suggest the presence of aqueous core within the PSs. Further to visualize the aqueous core of PSs, fluorescence microscopic images (Figure 4g–i) were obtained for these Cal-entrapped polymeric vesicle solutions. The intense green fluorescent spot in the images clearly indicate the existence of aqueous core within the PSs.

3.5. Hydrodynamic Size and Surface Charge of Polymersomes

DLS was used to measure mean hydrodynamic diameter (d_{H}) of the vesicular assemblies in aqueous media (pH 7). The size distribution profiles (Figure 5a) of all the polymer solutions are bimodal in nature. However, for both CP12 and CP13 polymers the size distribution is relatively narrow in comparison to CP11. For CP11, first peak and second peak appeared at around 9 nm and 150 nm, respectively. On the other hand, the first peak and second peak appear at around 25–27 nm and 170–180 nm, respectively

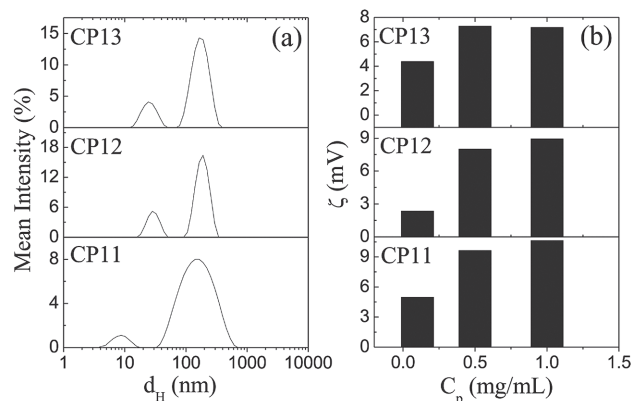
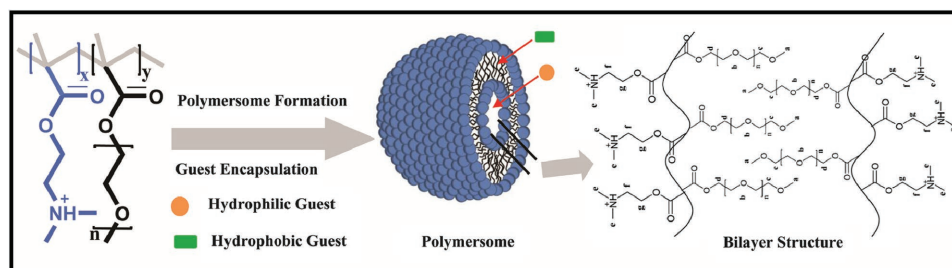


Figure 5. a) Hydrodynamic size distribution profiles (mean intensity versus average diameter, d_H , nm) of the PSs in different polymer solutions ($C_p = 1.0 \text{ mg mL}^{-1}$) at 298 K; b) bar graphs showing zeta potential (ζ/mV) values of different solutions (0.1, 0.5, and 1.0 mg mL^{-1}) of the copolymers **CP11**, **CP12**, and **CP13**.

for **CP12** and **CP13** polymers. The existence of aggregates of large size is consistent with the results of TEM and fluorescence measurements described above. In comparison to **CP12** and **CP13**, **CP11** exhibits broad size distribution for the larger aggregates and the mean d_H value of the aggregates is slightly less than 200 nm. This must be associated with relatively larger PDI value of polymer. However, as the aggregates are formed by inter-chain association, PDI cannot be correlated with the size distribution profile. Since the PSs have mean diameter of $\approx 200 \text{ nm}$, they will not show any potential threat to elimination via opsonization in the blood or through renal excretion.^[11,60]

The surface charge of the PSs in the employed range of polymer concentration was determined by zeta potential measurements. The data presented in Figure 5b show that the PSs are positively charged. As expected, with the increase of DMAEM content in the polymeric backbone the surface charge of the PSs increases. Since the DMAEM moiety only is responsible for the positive charge, during PS formation the DMAEM moieties project themselves toward the bulk water or toward aqueous core. In other words, the mPEG chains form the bilayer membrane of the PS as shown in Scheme 2.



Scheme 2. Schematic representations of vesicle formation by the copolymers **CP11**, **CP12**, and **CP13**; the representative bilayer structure showing probable interactions among mPEG chains.

3.6. Constitution of Bilayer Membrane

In support to the results of fluorescence and zeta potential measurements we performed NOESY (2-D) $^1\text{H-NMR}$ experiment for a representative polymer at $C_p > \text{CAC}$ in order to get an idea about the membrane structure of the PS. The NMR peaks in the NOESY spectrum (Figure S7, Supporting Information) were identified by use the corresponding $^1\text{H-NMR}$ spectrum (Figure S6, Supporting Information) of the polymer at $C_p > \text{CAC}$. The cross signals among the protons of the polymer clearly reveal interactions between (i) $-\text{OCH}_2\text{CH}_2\text{N}(\text{CH}_3)_2$ (g) and $-\text{OCH}_2\text{CH}_2\text{N}(\text{CH}_3)_2$ (f) protons, (ii) $-\text{OCH}_2\text{CH}_2\text{N}(\text{CH}_3)_2$ (g) and $-\text{OCH}_2\text{CH}_2\text{N}(\text{CH}_3)_2$ (e) protons, (iii) $-\text{OCH}_2\text{CH}_2\text{N}(\text{CH}_3)_2$ (f) and $-\text{OCH}_2\text{CH}_2\text{N}(\text{CH}_3)_2$ (e) protons of the DMAEM chain, and (iv) $-\text{OCH}_3$ (a) and $-\text{OCH}_2\text{CH}_2\text{O}-$ (b) protons of the mPEG chain. However, there is no such interaction between any of the protons of DMAEM chain and the $-\text{OCOCH}_2$ (d) or $-\text{CH}_2\text{OCH}_3$ (c) proton of the mPEG chain. The existence of these primary interactions leads to the conclusion that the DMAEM groups form the corona and mPEG chains constitute the bilayer membrane of the PS as shown in Scheme 2. However, since there are also some other interactions, for example, between (i) $-\text{OCH}_2\text{CH}_2\text{O}-$ (b) or $-\text{OCOCH}_2\text{CH}_2\text{O}-$ (d) protons of the mPEG chain and $-\text{OCH}_2\text{CH}_2\text{N}(\text{CH}_3)_2$ (g) protons of DMAEM chain, and (ii) $-\text{OCH}_2\text{CH}_2\text{O}-$ (b) protons of the mPEG chain and $-\text{OCH}_2\text{CH}_2\text{N}(\text{CH}_3)_2$ (f) or $-\text{OCH}_2\text{CH}_2\text{N}(\text{CH}_3)_2$ (e) protons of the DMAEM group, it is quite possible that some mPEG chains are also present among DMAEM chains forming the corona and thereby imparting structural stability to the PS by reducing the electrostatic repulsion among the positively charged head groups.

To further support our conclusion, we have performed a variable temperature (VT) $^1\text{H-NMR}$ experiment with **CP12** as a representative polymer in D_2O solvent. The $^1\text{H-NMR}$ spectrum (Figure 6) of the random copolymer at 25°C shows the characteristic signals of the protons ($-\text{OCH}_2\text{CH}_2\text{O}-$ and $-\text{OCH}_3$ groups) at 3.3–3.7 ppm corresponding to mPEG chain and the signals at 2.3 ppm ($\text{CH}_3-\text{N}-$) represent DMAEM group. The intensity of the peaks decreased when temperature is increased, resulting in broad signals due to the reduced flexibility of the

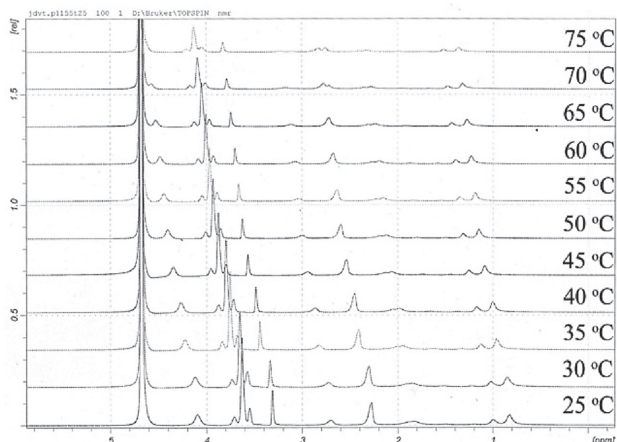


Figure 6. Temperature-dependent $^1\text{H-NMR}$ spectra of CP12 in D_2O (above CAC) showing ^1H signals of mPEG at 3.3–3.7 ppm and of DMAEM at 2.3–2.8 ppm in the temperature range 25–75 $^\circ\text{C}$.

polymer chains. But, it should be noted that the mPEG proton signals at 3.3–3.7 ppm decreased significantly in going from 25 to 60 $^\circ\text{C}$ in comparison to those of DMAEM signals at 2.3 and 2.7 ppm, suggesting the collapse of the mPEG chains with the gradual increase of temperature (Figure 6). This is consistent with literature reports,^[50–52] and suggests stronger interactions among the relatively less or completely dehydrated mPEG chains in the bilayer membrane of the PSs.

3.7. Thermal Stability of Polymersomes

Thermal stability of the polymeric DDS at elevated temperature is one of the important criteria for drug delivery application. In the VT $^1\text{H-NMR}$ experiment, the polymer solution in D_2O did not exhibit any turbidity even at 60 $^\circ\text{C}$, which means the LCST value of the mPEG chain-containing polymer is greater than 60 $^\circ\text{C}$, suggesting higher thermal stability of the PSs. It should be noted here that both the mPEG and DMAEM moieties of the polymer are temperature sensitive and DMAEM is also a pH-sensitive group.^[46,52,61] Since PEG is known to exhibit LCST, we performed turbidity (%T) measurements of the polymer solutions ($C_p = 1.0 \text{ mg mL}^{-1}$) at three different pHs (4, 7, and 9) in the temperature range of 25–75 $^\circ\text{C}$. The results are summarized in Figure 7a–c. Since mPEG chains constituting

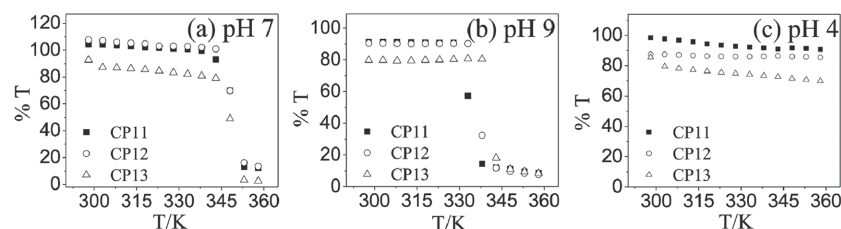


Figure 7. Variations of turbidity (%T, 400 nm) with temperature (T/K) of polymer (CP11, CP12, and CP13) solutions ($C_p = 1.0 \text{ mg mL}^{-1}$) at pH a) 7, b) 9, and c) 4.

the bilayer membrane are not in direct contact with the bulk water, the question of temperature-induced dehydration does not arise and therefore LCST phenomenon is not observed. This means dehydration of the DMAEM moieties only is responsible for the appearance of turbidity at higher temperatures. The plots in Figure 7a shows that the polymer solutions ($C_p = 1.0 \text{ mg mL}^{-1}$, pH 7) exhibit LCST above 75 $^\circ\text{C}$. This means that the copolymers are less likely to precipitate out at the physiological temperature (37 $^\circ\text{C}$). In other words, any premature release of the encapsulated cargo or blockage of the blood capillaries can be ruled out. The higher LCST value of these copolymers relative to those of typical hydrophobe-containing polymers is because of the highly polar and hence more hydrated DMAEM moieties that are in direct contact with the bulk water. The increase of interaction among DMAEM moieties as a result of dehydration upon increase of temperature causes phase separation of the polymers. This is confirmed by the lower LCST (<60 $^\circ\text{C}$) at pH 9.0 (Figure 7b) in which the $^+\text{NH}(\text{CH}_3)_2$ groups are either partially or fully deprotonated and therefore are less hydrated. On the other hand, at pH 4.0, all the $^+\text{NH}(\text{CH}_3)_2$ groups of DMAEM moieties being fully protonated, all the polymers become highly hydrated and consequently do not exhibit LCST phenomenon (Figure 7c). This means higher thermal stability of the polymer solutions in acidic environment. Thus based on the study of LCST phenomenon it can be concluded that the DMAEM moieties of the copolymers constitute the corona, while the mPEG chains are involved in forming the bilayer membrane of the PS.

3.8. pH-Induced Drug Release

Release of the encapsulated guest at the target site is also an important parameter for a good DDS. pH is one of major stimuli for release of encapsulated cargo from a DDS. Since these PSs have ionic functionalities as head group with hydrolysable ester bonds, pH can be a good stimulus for the release of encapsulated guest as in several other cases.^[52,56,57] Cal is a pH-sensitive fluorescent dye and its fluorescence intensity is known to decrease with the increase as well as decrease of pH of the medium.^[62] Therefore, the release of PS-encapsulated Cal dye upon reduction of pH of the polymer solutions was investigated.

Fluorescence spectra (Figure 8a–c) of Cal in the polymer solutions (0.2 mg mL^{-1}) of different pH were measured after 1 h of incubation. At pH 7 and 8, all the PSs have shown more or less same maximum intensity, indicating similar encapsulation efficiency. That is no destabilization or disintegration of the PSs was observed in these pHs. However, in more acidic conditions (e.g., at pH =

5 and 4), the fluorescence intensity of Cal decreased to a large extent for all the polymers. Since under acidic condition, the PSs showed a burst release of the Cal, it rules out the possibility of slow diffusion of the guest from the PSs or time-dependent hydrolysis of the ester linkages in the DMAEM and/or mPEG chains. Also the polymers become highly positively charged in acidic pH, which may destabilize the PSs due to increased electrostatic repulsion among the cationic $^+\text{NH}(\text{CH}_3)_2$ groups on the surface, leading to a burst release of the guest. Such kind of burst release of drug from the PSs can be successfully used for the treatment of solid tumors.

Since in acidic pH, the PSs have a tendency to release the encapsulated guest from their aqueous core, there might be an associated change of the morphology of the molecular self-assemblies formed by these copolymers. Therefore, HRTEM images of the polymer solutions in pH 4 buffer were taken. The TEM pictures in Figure 8d–f clearly reveal the presence of polymeric micelles instead of any PSs. In acidic pH, there will be an additional protonation of the tertiary amine group, which is responsible for the transformation of the PSs present in pH 7 to nearly spherical polymeric micelles of comparatively bigger sizes (≈ 100 nm) in pH 4 buffer. DLS study of the polymer solution ($C_p = 0.1\%$) at pH 4 also supports the HRTEM images (Figure 8g–i), showing an overall increase in d_H of the polymeric micelles in each of the copolymer solutions.

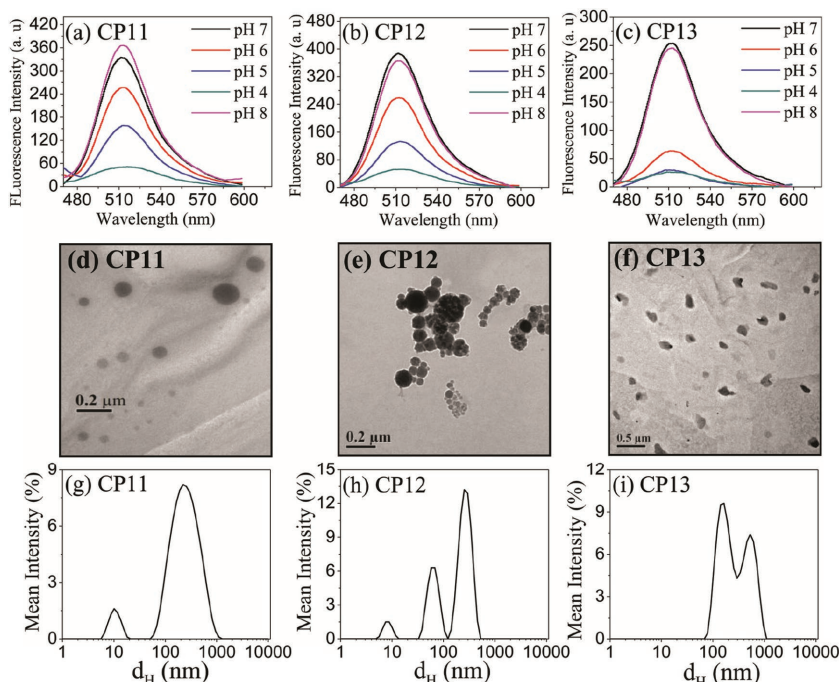


Figure 8. a–c) Fluorescence spectra of Cal in different polymer (CP11, CP12, CP13) solutions ($C_p = 0.2$ mg mL $^{-1}$) at different pH of the medium after 1 h of incubation; d–f) HRTEM images (200 kV) of the polymer solutions ($C_p = 1.0$ mg mL $^{-1}$) at pH 4; g–i) hydrodynamic size distribution profiles for the copolymer solutions ($C_p = 1.0$ mg mL $^{-1}$) at pH 4.

For **CP13** also, the existence of ill-defined nanostructures is supported by the irregular size distribution profile. The cationic polymers experience more electrostatic repulsion and consequently form relatively less compact micellar type aggregates with large hydrodynamic diameter.^[63] Thus, the hydrophilic dye release from the PSs in acidic pH is well supported by the concomitant change of morphology from PS to polymeric micelles.

3.9. Hemocompatibility of Polymers

Hemocompatibility or hemolysis study is very important for all foreign materials to be used as intravenous (i.v.) DDS. Therefore, the assay was performed by collecting RBCs from blood. The percentage of hemolysis of RBCs at various concentrations ($C_p = 0.5$ to 2.0 mg mL $^{-1}$) of polymers is shown by the bar graph in Figure 9a. For comparison purposes, the data for negative (RBCs suspended in PBS) as well as positive (RBCs suspended in 1% triton X-100) controls are also included. From the graph, it is very much evident that all the polymers are highly hemocompatible at moderate to high concentrations. Their hemolysis is very much comparable to the negative control. This negligible amount of hemolysis can be attributed to the absence of any typical hydrophobe in the polymeric backbone. This high level of hemocompatibility is encouraging for all three copolymers as intravenous DDS.

3.10. Cell Viability Study

Cytotoxicity is an important parameter for a DDS for authentic application. As per previous reports, poly[DMAEM] and polymers containing poly[DMAEM] block are responsible for sufficient level of cytotoxicity and their toxicity increased with the increase of DMAEM part in their polymeric backbone.^[45,64] Therefore, an extensive cytotoxicity study at different polymer concentrations was carried out using breast cancer cells (MDA-MB-231). The results presented in Figure 9b are indicative of highly biocompatible nature of all three copolymers. But the cell viability slightly deteriorated in the case of **CP11** polymer at the highest concentration (1.0 mg mL $^{-1}$), which might be due to the overall increase of DMAEM content or to the positive charge in the polymer side chain beyond its tolerance level in comparison to **CP12** and **CP13** polymers. The overall low cytotoxicity for these polymers at this elevated level



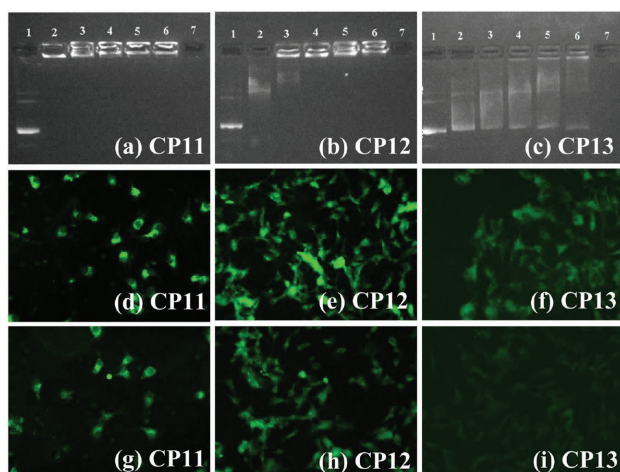


Figure 11. a–c) Gel retardation assay validating condensation of the pDNA with cationic polymers. Lanes 1 and 7 are only pDNA and polymer as control, respectively. The DNA–polymer complexes were made in the ratios 1:10, 1:25, 1:50, 1:100, 1:200 and loaded in lanes 2, 3, 4, 5, 6, respectively. Each DNA–polymer complex was incubated for 1 h before loading. CFM images of MDA-MB-231 cells transfected by different weight ratios: d–f) 1:100 and g–i) 1:50 of pDNA/polymer complexes.

suggesting utilization of these PSs as potential codelivery system.

Though all the copolymers were found to be biocompatible up to a reasonably high concentration and pDNA used for this study is widely accepted, it is important to check the cytocompatibility of the polyplex, i.e., polymer after complexation with the pDNA. Therefore, *in vitro* cell viability study on the breast cancer cell line (MDA-MB-231 cells) was performed and the results are summarized in Figure S10 (Supporting Information). It is interesting to observe that toxicity of the polyplexes is similar to the pure copolymer (see Figure 9b). Only for CP13 and at higher concentration of CP11, there is a slight deterioration of the cell viability in comparison to the polymer itself. Thus overall, all these polyplexes are cytocompatible and can be used for gene transfection.

3.13. In Vitro Gene Transfection

Transfection experiments were performed on MDA-MB-231 cells using a plasmid containing reporter gene encoding GFP. The weight ratios (pDNA:polymer as 1:50 and 1:100), at which DNA retardation was observed, were used for transfection study. The results are summarized in Figure 11d–i. The green fluorescence from transfected breast cancer cells clearly indicates a reporter gene expression. It can be observed that qualitatively the transfection efficiency increased in each case when higher weight ratio of the pDNA/polymer complexes was employed. Also the overall the transfection is evidently higher for CP11 and CP12 copolymers in comparison to CP13. Since the CP11

polymer is less biocompatible compared to CP12 and CP13, at higher polymer concentrations of CP11, the cells become slightly deformed. Thus it can be concluded that CP12 holds the best gene transfection ability among these three positively charged copolymers.

4. Conclusions

In summary, three random cationic copolymers having different mole ratios of DMAEM and mPEG were synthesized and characterized. All three copolymers exhibit surface activity and spontaneously form PSs without the need of any external stimuli or organic solvent. Though mPEG chains are known to be polar in character, this study demonstrates that the mPEG chains behave like hydrocarbon tails of conventional surfactants and constitute the bilayer membrane of the PSs. In fact, this is one of the few reports on PS formation by random copolymers. Importantly, PS formation takes place at room temperature which is an advantage over previously reported DMAEM and mPEG based PSs that formed at higher temperature.^[50] The size and shapes of the PSs have been well corroborated with the DDSs. The absence of any LCST phenomenon in the temperature range of 25–60 °C at neutral pH confirmed stability of the PSs at physiological temperature (37 °C). However, the cationic PSs become less stable at acidic pH, showing their pH-sensitivity. Therefore, the PSs could not only encapsulate hydrophilic model drug (Cal and R6G dyes) in their nanostructure at pH 7, but also exhibited a pH-triggered release of the hydrophilic guest from the aqueous lumen of the PSs as a result of vesicle-to-micelle transition at acidic pH. All the copolymers were found to be highly hemocompatible and no denaturing effect on the blood circulatory protein HSA was observed even at a relatively high polymer concentration. The existence of intact PSs in the presence of serum albumin and pDNA proves robustness of the vesicles necessary for *in vivo* applications. Further, all copolymers were found to be highly cell viable or nontoxic up to a relatively high concentration. This is an obvious advantage over PEI-based (linear and branched) gene delivery systems.^[67] All three copolymers exhibited DNA condensing ability, which increased with the increase of the positive charge carrying DMAEM functionality in the polymeric backbone. The CP12 polymer showed best transfection ability than CP11 and CP13 on breast cancer cell line. Like PEI, the transfection ability of the polymers proves their efficient endosomal escape ability before protein expression.^[67,68] Overall, all these easily made random cationic polymers could be an efficient competitor to synthetically more challenging knot^[31] or highly branched poly(β -amino ester)s^[33] or block cationic polymers,^[35] and also to lipoplex-based delivery systems^[69,70] due to higher stability of the polyplexes. Possible utilization as potential



codelivery system for drugs (hydrophobic as well as hydrophilic) and genetic materials makes these polymers more attractive over only gene delivery systems, such as PEI and PLL as nonviral vector.^[70] It should also be noted that like peptide bonds in PLL, the presence of ester bonds in the polymer structure makes the copolymers more biodegradable than PEI (linear or branched).^[70]

Supporting Information

Supporting Information is available from the Wiley Online Library or from the author.

Acknowledgements: The authors gratefully acknowledge the Department of Science and Technology, New Delhi for financial support (Grant no. SR/S1/PC-68/2008) of this work. P.L. thanks CSIR, New Delhi (no. 20-06/2010 (i) EU-IV) for a research fellowship.

Received: August 1, 2016; Revised: October 15, 2016;
Published online: ; DOI: 10.1002/mabi.201600324

Keywords: biocompatibility; cationic polymersomes; gene transfection; pH-sensitive drug delivery; random copolymers

- [1] L. Li, K. Raghupathi, C. Song, P. Prasad, S. Thayumanavan, *Chem. Commun.* **2014**, *50*, 13417.
- [2] Y. Mai, A. Eisenberg, *Chem. Soc. Rev.* **2012**, *41*, 5969.
- [3] A. Blanz, N. J. Warren, A. L. Lewis, S. P. Armes, A. J. Ryan, *Soft Matter* **2011**, *7*, 6399.
- [4] R. Hoogenboom, S. Rogers, A. Can, C. R. Becer, C. Guerrero-Sanchez, D. Wouters, S. Hoepfner, U. S. Schubert, *Chem. Commun.* **2009**, *37*, 5582.
- [5] C. C. Müller-Goymann, *Eur. J. Pharm. Biopharm.* **2004**, *58*, 343.
- [6] M. Licciardi, G. Giammona, J. Du, S. P. Armes, Y. Tang, A. L. Lewis, *Polymer* **2006**, *47*, 2946.
- [7] Z. Ge, S. Liu, *Chem. Soc. Rev.* **2013**, *42*, 7289.
- [8] C. Monfardini, F. M. Veronese, *Bioconjugate Chem.* **1998**, *9*, 418.
- [9] A. Vonarbourg, C. Passirani, P. Saulnier, J. P. Benoit, *Biomaterials* **2006**, *27*, 4356.
- [10] R. Tong, L. Tang, L. Ma, C. Tu, R. Baumgartner, J. Cheng, *Chem. Soc. Rev.* **2014**, *43*, 6982.
- [11] F. Meng, Z. Zhong, J. Feijen, *Biomacromolecules* **2009**, *10*, 197.
- [12] J. Du, R. K. O'Reilly, *Soft Matter* **2009**, *5*, 3544.
- [13] B. M. Discher, Y. Y. Won, D. S. Ege, J. C. Lee, F. S. Bates, D. E. Discher, D. A. Hammer, *Science* **1999**, *284*, 1143.
- [14] P. J. Photos, L. Bacakova, B. Discher, F. S. Bates, D. E. Discher, *J. Controlled Release* **2003**, *90*, 323.
- [15] D. E. Discher, F. Ahmed, *Annu. Rev. Biomed. Eng.* **2006**, *8*, 323.
- [16] J. Du, L. Fan, Q. Liu, *Macromolecules* **2012**, *45*, 8275.
- [17] R. P. Brinkhuis, F. P. Rutjes, J. C. van Hest, *Polym. Chem.* **2011**, *2*, 1449.
- [18] K. Kita-Tokarczyk, J. Grumelard, T. Haefele, W. Meier, *Polymer* **2005**, *46*, 3540.
- [19] W. Chen, F. Meng, R. Cheng, Z. Zhong, *J. Controlled Release* **2010**, *142*, 40.
- [20] J. Rodríguez-Hernández, S. Lecommandoux, *J. Am. Chem. Soc.* **2005**, *127*, 2026.
- [21] M. A. Ward, T. K. Georgiou, *Polymers* **2011**, *3*, 1215.
- [22] L. Jia, D. Cui, J. Bignon, A. Di Cicco, J. Wdzieczak-Bakala, J. Liu, M. H. Li, *Biomacromolecules* **2014**, *15*, 2206.
- [23] F. Checot, S. Lecommandoux, H. A. Klok, Y. Gnanou, *Eur. Phys. J. E: Soft Matter* **2003**, *10*, 25.
- [24] W. Gao, J. M. Chan, O. C. Farokhzad, *Mol. Pharmaceutics* **2010**, *7*, 1913.
- [25] D. Putnam, C. A. Gentry, D. W. Pack, R. Langer, *Proc. Natl. Acad. Sci. USA* **2001**, *98*, 1200.
- [26] S. Zhang, B. Zhao, H. Jiang, B. Wang, B. Ma, *J. Controlled Release* **2007**, *123*, 1.
- [27] D. J. Gary, N. Puri, Y. Y. Won, *J. Controlled Release* **2007**, *121*, 64.
- [28] H. Y. Cho, S. E. Averick, E. Paredes, K. Wegner, A. Averick, S. Jurga, K. Matyjaszewski, *Biomacromolecules* **2013**, *14*, 1262.
- [29] D. Zhou, L. Cutlar, Y. Gao, W. Wang, J. O'Keeffe-Ahern, S. McMahon, B. Duarte, F. Larcher, B. J. Rodriguez, U. Greiser, W. Wang, *Sci. Adv.* **2016**, *2*, 1.
- [30] D. Zhou, Y. Gao, A. Aied, L. Cutlar, O. Igoucheva, B. Newland, V. Alexeeve, U. Greiser, J. Uitto, W. Wang, *J. Controlled Release*, DOI: 10.1016/j.jconrel.2016.06.014.
- [31] L. Cutlar, Y. Gao, A. Aied, U. Greiser, E. M. Murauer, D. Zhou, W. Wang, *Biomater. Sci.* **2016**, *4*, 92.
- [32] J. Y. Huang, Y. Gao, L. Cutlar, J. O'Keeffe-Ahern, T. Zhao, F. H. Lin, D. Zhou, S. McMahon, U. Greiser, W. Wang, W. Wang, *Chem. Commun.* **2015**, *51*, 8473.
- [33] L. Cutlar, D. Zhou, Y. Gao, T. Zhao, U. Greiser, W. Wang, W. Wang, *Biomacromolecules* **2015**, *16*, 2609.
- [34] L. Cutlar, D. Zhou, X. Hu, B. Duarte, U. Greiser, F. Larcher, W. Wang, *Exp. Dermatol.*, **2016**, *25*, 818.
- [35] C. Zhu, S. Jung, S. Luo, F. Meng, X. Zhu, T. G. Park, Z. Zhong, *Biomaterials* **2010**, *31*, 2408.
- [36] Y. Wang, S. Gao, W. H. Ye, H. S. Yoon, Y. Y. Yang, *Nat. Mater.* **2006**, *5*, 791.
- [37] Q. Tang, B. Cao, G. Cheng, *Chem. Commun.* **2014**, *50*, 1323.
- [38] J. Zhang, L. Wu, F. Meng, Z. Wang, C. Deng, H. Liu, Z. Zhong, *Langmuir* **2012**, *28*, 2056.
- [39] N. Wiradharma, Y. Zhang, S. Venkataraman, J. L. Hedrick, Y. Y. Yang, *Nano Today* **2009**, *4*, 302.
- [40] J. Ding, C. Xiao, C. He, M. Li, D. Li, X. Zhuang, X. Chen, *Nanotechnology* **2011**, *22*, 494012.
- [41] V. A. Vasanth, S. Jana, S. S. C. Lee, C. S. Lim, S. L. M. Teo, A. Parthiban, J. G. Vancso, *Polym. Chem.* **2015**, *6*, 599.
- [42] J. Zhou, F. Ke, Y. Y. Tong, Z. C. Li, D. Liang, *Soft Matter* **2011**, *7*, 9956.
- [43] H. Bao, L. Li, L. H. Gan, Y. Ping, J. Li, P. Ravi, *Macromolecules* **2010**, *43*, 5679.
- [44] M. Spasova, L. Mespouille, O. Coulembier, D. Paneva, N. Manolova, I. Rashkov, P. Dubois, *Biomacromolecules* **2009**, *10*, 1217.
- [45] Y. Qiao, Y. Huang, C. Qiu, X. Yue, L. Deng, Y. Wan, J. Xing, C. Zhang, S. Yuan, A. Dong, J. Xu, *Biomaterials* **2010**, *31*, 115.
- [46] S. H. Yuk, S. H. Cho, S. H. Lee, *Macromolecules* **1997**, *30*, 6856.
- [47] F. L. Baines, S. P. Armes, N. C. Billingham, Z. Tuzar, *Macromolecules* **1996**, *29*, 8151.
- [48] X. Yue, Y. Qiao, N. Qiao, S. Guo, J. Xing, L. Deng, J. Xu, A. Dong, *Biomacromolecules* **2010**, *11*, 2306.
- [49] C. L. Peng, H. M. Tsai, S. J. Yang, T. Y. Luo, C. F. Lin, W. J. Lin, M. J. Shieh, *Nanotechnology* **2011**, *22*, 265608.

- [50] C. Pietsch, U. Mansfeld, C. Guerrero-Sanchez, S. Hoepfner, A. Vollrath, M. Wagner, R. Hoogenboom, S. Saubern, S. H. Thang, C. R. Becer, J. Chiefari, U. S. Schubert, *Macromolecules* **2012**, *45*, 9292.
- [51] J. Dey, S. Shrivastava, *Langmuir* **2012**, *28*, 17247.
- [52] P. Laskar, J. Dey, S. K. Ghosh, *Colloids Surf. B* **2016**, *139*, 107.
- [53] H. X. Zhang, E. Liu, *J. Inclusion Phenom. Macrocyclic Chem.* **2012**, *74*, 231.
- [54] U. Anand, C. Jash, S. Mukherjee, *J. Phys. Chem. B* **2010**, *114*, 15839.
- [55] E. Froehlich, J. S. Mandeville, C. J. Jennings, R. Sedaghat-Herati, H. A. Tajmir-Riahi, *J. Phys. Chem. B* **2009**, *113*, 6986.
- [56] P. Laskar, S. Samanta, S. K. Ghosh, J. Dey, *J. Colloid Interface Sci.* **2014**, *430*, 305.
- [57] P. Laskar, B. Saha, S. Ghosh, J. Dey, *RSC Adv.* **2015**, *5*, 16265.
- [58] F. Li, G. Z. Li, H. Q. Wang, Q. J. Xue, *Colloid Surf., A* **1997**, *127*, 89.
- [59] E. N. Savariar, S. V. Aathimankandan, S. Thayumanavan, *J. Am. Chem. Soc.* **2006**, *128*, 16224.
- [60] J. S. Lee, J. Feijen, *J. Controlled Release* **2012**, *161*, 473.
- [61] D. Fournier, R. Hoogenboom, H. M. Thijs, R. M. Paulus, U. S. Schubert, *Macromolecules* **2007**, *40*, 915.
- [62] B. Maherani, E. Arab-Tehrany, A. Kheirloom, D. Geny, M. Linder, *Biochimie* **2013**, *95*, 2018.
- [63] C. Maiti, R. Banerjee, S. Maiti, D. Dhara, *Langmuir* **2015**, *31*, 32.
- [64] P. van de Wetering, E. E. Moret, N. M. Schuurmans-Nieuwenbroek, M. J. van Steenberg, W. E. Hennink, *Bioconjugate Chem.* **1999**, *10*, 589.
- [65] K. H. Delgado-Magnero, P. A. Valiente, M. Ruiz-Peña, A. Pérez-Gramatges, T. Pons, *Colloids Surf., B* **2014**, *116*, 720.
- [66] H. Zhu, C. Dong, H. Dong, T. Ren, X. Wen, J. Su, Y. Li, *ACS Appl. Mater. Interfaces* **2014**, *6*, 10393.
- [67] D. Putnam, C. A. Gentry, D. W. Pack, R. Langer, *Proc. Natl. Acad. Sci. USA* **2001**, *98*, 1200.
- [68] R. Goyal, S. K. Tripathi, E. Vazquez, P. Kumar, K. C. Gupta, *Bio-macromolecules* **2011**, *13*, 73.
- [69] M. Ramamoorth, A. Narvekar, *J. Clin. Diagn. Res.* **2015**, *9*, GE01.
- [70] H. Eliyahu, Y. Barenholz, A. J. Domb, *Molecules* **2005**, *10*, 34.